Journal of
Materials Chemistry B

PAPER

View Article Online
View Journal | View Issue

Cite this: J. Mater. Chem. B, 2016, 4, 4934

Pyrano[3,2-c]julolidin-2-ones: a novel class of fluorescent probes for ratiometric detection and imaging of Hg^{2+} in live cancer cells†

Ajay Kumar Jha,[a] Shahida Umar,[a] Rakesh Kumar Arya,[b] Dipak Datta[b] and Atul Goel*[ac]

Received 7th June 2016,
Accepted 17th June 2016

DOI: 10.1039/c6tb01413e

www.rsc.org/MaterialsB

A novel pyrano[3,2-c]julolidin-2-one based fluorescent molecular rotor **PYJO4** has been designed and developed for selective ratiometric detection, quantification and imaging of intracellular Hg^{2+} in live cells. The probe operates *via* a Twisted Intramolecular Charge Transfer (TICT) mechanism and exhibits high selectivity and sensitivity up to 1.14 ppb. **PYJO4** coated test strips can be used to detect mercury ions in contaminated water.

Introduction

Mercury, exhibiting an anomalous property of being 'liquid metal' in its native form, acts as one of the most toxic and disastrous elements.[1] It causes serious environmental and health problems as the aquatic organisms convert the inorganic mercury into neurotoxic methyl mercury which bio-accumulates through the food chain leading to disasters like Minamata.[1] Furthermore, dental amalgam which consists of approximately 50% mercury content can seriously affect the central nervous system leading to the risk of neurodegenerative disorders.[2] Hence, there is an urge to develop fluorescent probes that can detect intracellular Hg^{2+} ions with high selectivity and sensitivity.

Most of the current Hg^{2+} sensors known in the literature rely on single intensity based measurements *via* either turn-on[3] or turn-off[4] responses. However, their responses depend on the concentration of the sensor, source light intensity, and sensitivity of the analytical instrument which may lead to unintentional variability in readouts during measurements.[3] To overcome these limitations, dual-intensity based (ratiometric) fluorescent probes with metal ion selectivity are in huge demand as they offer accuracy with high precision and inbuilt calibration.[5] Lippard *et al.*[6a] developed the first ratiometric fluorescent sensor for Hg^{2+} ions and since then very few ratiometric fluorescent probes for Hg^{2+} ions have been reported but they are either non-selective or exhibit excitation in the ultra-violet region thus restricting their application in live cell imaging.[6] Later in the year 2008, Zhang *et al.*[6d] reported the first FRET-based ratiometric imaging of Hg^{2+} ions in cancer cells. They highlighted that ratiometric sensors can be designed to work mainly by two mechanisms, *viz.* intramolecular charge transfer (ICT) and fluorescence resonance energy transfer (FRET). The reaction based sensors (chemodosimeters) in general follow an irreversible binding mechanism, thus limiting their applications. We envision that an alternative strategy for designing ratiometric sensors with significant accuracy may be achieved by the twisted-ICT (TICT) approach. The TICT concept[7] of molecular rotors has been scarcely explored possibly due to the difficulty in delicately correlating the degree of electron transfer to the change in molecular geometry during metal binding.

These molecular rotors,[8] having a donor–π–acceptor framework, adopt a twisted state upon photoexcitation and can relax to the ground state from their photo-excited state either non-radiatively or by a red-shifted emission band leading to dual emission bands belonging to the locally excited (LE) and TICT states. In this paper, we rationally designed (Fig. 1) and synthesized a novel dialkylamino-nitrile appended pyranojulolidin-2-one probe attached to a metal ion acceptor dipicolylamine[9] (DPA) for ratiometric detection and imaging of Hg^{2+} ions in live cancer cells. The main features of our probe include a TICT-based novel pyrano[3,2-c]julolidin-2-one fluorophore, selective ratiometric detection, and quantification and imaging of intracellular Hg^{2+} in live cells with nano-molar sensitivity. In this paper, we have also demonstrated a convenient test strip method for the detection of Hg^{2+} ions in aqueous solution. The advantages of our probe over existing ratiometric Hg^{2+} probes are summarized in Table S1 (ESI†).

[a] Fluorescent Chemistry Lab, Department of Medicinal and Process Chemistry, CSIR-Central Drug Research Institute, Lucknow 226031, India. E-mail: atul_goel@cdri.res.in
[b] Biochemistry Division, CSIR-Central Drug Research Institute, Lucknow 226031, India
[c] Academy of Scientific and Innovative Research, New Delhi 110001, India

† Electronic supplementary information (ESI): Synthesis, characterization and experimental data. See DOI: 10.1039/c6tb01413e

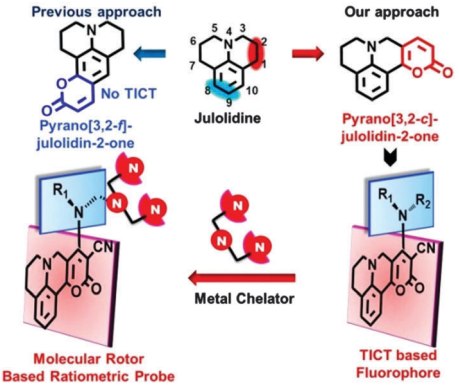

Fig. 1 A new strategy for developing a TICT based ratiometric probe.

Materials and methods

Instruments

^{1}H NMR spectra were recorded at 400 MHz or 500 MHz and ^{13}C NMR spectra were recorded at 100.6 MHz. Chemical shifts are reported in parts per million shift (δ-value) from Me_4Si (δ 0 ppm for ^{1}H) or based on the middle peak of the solvent ($CDCl_3$) (δ 7.26 ppm for ^{1}H NMR and δ 77.00 ppm for ^{13}C NMR)/DMSO-d_6 (δ 2.50 ppm for ^{1}H NMR and δ 40.00 ppm for ^{13}C NMR) as an internal standard. Signal patterns are indicated as s, singlet; d, doublet; t, triplet; m, multiplet. The coupling constant (J) is given in Hertz. Infrared (IR) spectra were recorded in a KBr disc and reported in wave number (cm^{-1}). The ESI-MS spectra were recorded on a MICROMASS Quadro-II LCMS system. The HRMS spectra were recorded as ESI-HRMS on a mass analyzer system. All the reactions were monitored by TLC and visualization was done with UV light (254 nm).

Synthesis

Synthesis of compound 2. To an ice-chilled solution of sodium hydride (10.08 g, 60% oil suspension, 0.42 mol) in THF, methyl cyanoacetate (35.2 mL, 0.4 mol) was added dropwise for a period of 15 min. After complete addition of methyl cyanoacetate, the resulting white semi-solid material was vigorously stirred for another 15 min. To this solution, carbon disulfide (25.33 mL, 0.4 mol) was added dropwise while the mixture was kept below 20 °C. The reaction mixture was slowly changed from white semisolid to yellow liquid. Methyl iodide (62.55 mL, 1 mol) was added dropwise to the stirred solution over a period of 30 min. After the mixture was stirred for another 15 min at room temperature, THF was removed under reduced pressure. A small amount of crushed ice was added to consume unreacted NaH and then the residue was poured into ice-cold water with constant stirring. The white crystalline compound was filtered, washed with cold water, dried and recrystallized with ethyl acetate–hexane (1 : 4) to obtain white needles. Yield: 89%; m.p.: 52–53 °C.[10]

Synthesis of compound 3 (PYJO1). A mixture of methyl-2-cyano-3,3-dimethylsulfanylacrylate **2** (203 mg, 1 mmol, 1 equiv.), julolidin-1-one **1** (206 mg, 1.1 mmol, 1.1 equiv.) and NaH (48 mg, 2 mmol, 2 equiv.) in DMF (20 mL) was stirred at room temperature for 24 h. After completion, the reaction mixture was poured into ice water with constant stirring. The precipitate thus obtained was filtered and purified on a silica gel column using chloroform as the eluent to afford 240 mg (77%) of **PYJO1** as a violet solid; R_f = 0.55 (chloroform/methanol, 10 : 1, v/v); m.p. (chloroform/methanol) 178–180 °C; MS (ESI) 311 $[M + H]^+$; IR (KBr) ν = 2212, 1735 cm^{-1}; ^{1}H NMR (400 MHz, $CDCl_3$): δ 7.37–7.59 (m, 1H), 6.90–7.12 (m, 1H), 6.61 (t, J = 7.64 Hz, 1H,), 4.32 (s, 2H), 3.14 (t, J = 5.54 Hz, 2H), 2.97 (s, 3H), 2.71 (t, J = 6.24, 2H), 1.89–2.15 (m, 2H), ppm; ^{13}C NMR (100.6 MHz, $CDCl_3$): δ = 164.6, 158.5, 154.5, 145.4, 134.2, 123.6, 122.6, 117.7, 115.4, 112.0, 105.9, 91.0, 49.4, 48.9, 26.6, 20.8, 17.4 ppm; HRMS calculated for $C_{17}H_{15}N_2O_2S$ $[M + H]^+$ 311.0854, found: 311.0856.

Synthesis of compound 4 (PYJO2). Compound 4-(methylthio)-2-oxo-2*H*-pyrano[3,2-*c*]julolidine-3-carbonitrile (**PYJO1**) (310 mg, 1 mmol, 1 equiv.) was refluxed in THF with 2-(methylamino)-ethanol (90 μL, 1.2 mmol, 1.2 equiv.) for 6–7 h, and the reaction mixture was cooled to room temperature and was filtered. The precipitate thus obtained was purified on a silica gel column with 1% methanol in chloroform as the eluent to afford 263 mg (78%) of **PYJO2** as a red solid; R_f = 0.45 (chloroform/methanol, 10:2, v/v); m.p. (chloroform/methanol) 196–198 °C; MS (ESI) 338 $[M + H]^+$; IR (KBr) ν = 2210, 1742 cm^{-1}; ^{1}H NMR (400 MHz, DMSO-d_6): δ 7.17–7.39 (m, 1H), 6.94–7.16 (m, 1H), 6.66 (t, J = 7.58 Hz, 1H), 4.86 (t, 1H, J = 5.12 Hz), 4.15 (s, 2H), 3.54–3.76 (m, 2H), 3.34–3.57 (m, 2H), 3.01–3.28 (m, 5H), 2.56–2.78 (m, 2H), 1.79–2.02 (m, 2H), ppm; ^{13}C NMR (100.6 MHz, $CDCl_3$): δ = 166.7, 161.2, 154.8, 145.4, 133.3, 123.4, 122.5, 118.0, 117.7, 114.4, 104.3, 78.4, 58.5, 57.8, 49.1, 49.0, 41.1, 26.4, 21.0 ppm; HRMS calculated for $C_{19}H_{20}N_3O_3$ $[M + H]^+$ 338.1505, found: 338.1489.

Synthesis of compound 5 (PYJO3). A mixture of 4-((2-hydroxyethyl)(methyl)amino)-2-oxo-2*H*-pyrano[3,2-*c*]julolidine-3-carbonitrile (**PYJO2**) (337 mg, 1 mmol, 1 equiv.), 4-dimethylaminopyridine (DMAP) (146 mg, 1.2 mmol, 1.2 equiv.) and 2-chloroacetyl chloride (280 mg, 2.5 mmol, 2.5 equiv.) in dry DCM (25 mL) was stirred at room temperature for 30 min, and then refluxed for another 3 h. The mixture was then cooled down, poured into 30 mL of ice water and further extracted with DCM and the organic layer was dried over anhydrous Na_2SO_4, and purified on a silica gel column with 1% methanol in chloroform as the eluent to afford 340 mg (82%) of **PYJO3** as a red solid R_f = 0.45 (chloroform/methanol, 10 : 1, v/v); m.p. (chloroform/methanol) 168–170 °C; MS (ESI) 414 $[M + H]^+$, 416 $[M + 2 + H]^+$; IR (KBr) ν = 2211, 1742 cm^{-1}; ^{1}H NMR (400 MHz, $CDCl_3$): δ 7.40–7.62 (m, 1H) 6.93–7.15 (m, 1H), 6.68 (t, J = 7.64 Hz, 1H), 4.47 (t, J = 5.12 Hz, 2H), 3.95–4.18 (m, 4H), 3.74 (t, J = 5.08 Hz, 2H,), 3.04–3.28 (m, 5H), 2.73 (t, J = 6.30 Hz, 2H) 1.90–2.16 (m, 2H) ppm; ^{13}C NMR (100.6 MHz, $CDCl_3$): δ = 167.3, 160.6, 157.0, 145.0, 133.6, 123.3, 123.0, 118.2, 116.3, 114.1, 103.3, 82.1, 61.9, 53.5, 49.7, 49.1, 40.8, 40.5, 26.4, 21.0 ppm; HRMS calculated for $C_{21}H_{21}ClN_3O_4$ $[M + H]^+$ 414.1221, found: 414.1211, $[M + 2 + H]^+$ 416.1191, found 416.1184.

Synthesis of compound 6 (PYJO4). A mixture of 2-((3-cyano-2-oxo-2*H*-pyrano[3,2-*c*]julolidinyl)(methyl)amino)ethyl-2-chloroacetate (**PYJO3**) (413 mg, 1 mmol, 1 equiv.), di-(2-picolyl)amine (DPA) (198 mg, 1 mmol), *N*,*N*-diisopropylethylamine (DIPEA) (0.5 mL), and potassium iodide (30 mg) in acetonitrile (50 mL)

was refluxed for 8 h. The mixture was cooled to room temperature, and the solvent was removed under reduced pressure to obtain red oil, which was dissolved in CH_2Cl_2 (150 mL). The organic layer was dried over anhydrous Na_2SO_4, and purified on a silica gel column with 2% methanol in chloroform as the eluent to afford 403 mg (70%) of **PYJO4** as a red solid; R_f = 0.42 (chloroform/methanol, 10 : 2, v/v); m.p. (chloroform/methanol) 70–72 °C; MS (ESI) 577 $[M + H]^+$; IR (KBr) ν = 2209, 1740 cm^{-1}; ^1H NMR (400 MHz, $CDCl_3$): δ 8.33–8.61 (m, 2H), 7.34–7.73 (m, 5H), 6.89–7.24 (m, 3H), 6.53–6.76 (m, 1H), 4.27–4.49 (m, 2H), 3.84–4.12 (m, 6H), 3.58–3.70 (m, 2H), 3.47 (s, 2H), 2.97–3.26 (m, 5H), 2.57–2.70 (m, 2H), 1.84–2.06 (m, 2H) ppm; ^{13}C NMR (100.6 MHz, $CDCl_3$): δ 170.8, 166.8, 160.6, 158.3, 156.4, 148.8, 148.7, 144.8, 136.4, 133.2, 123.0, 122.0, 117.7, 116.2, 113.8, 103.0, 81.0, 60.3, 59.5, 54.3, 53.6, 49.3, 48.9, 40.7, 26.2, 20.7 ppm; HRMS calculated for $C_{33}H_{33}N_6O_4$ $[M + H]^+$ 577.2563, found: 577.2553.

Photophysical (absorption and emission) studies

Triple distilled water (TDW) was used for preparing all analytical samples. Parent stock solutions (2.5 mM) of the perchlorate salts of all metal ions and synthesized pyranojulolidine derivatives **PYJO1**, **PYJO2**, **PYJO3**, and **PYJO4** (4×10^{-4} M) were prepared in analytical grade methanol. The absorption and fluorescence spectra for metal sensing experiments were obtained after analyte addition at 25 °C under 405 nm excitation in methanol/HEPES (7 : 3 (v/v), 20 mM, pH 7.2).

TDDFT study of probe PYJO4

To study the electronic behaviour of **PYJO4** time-dependent density functional theory (TDDFT) calculations were performed using the Gaussian 09 package.[11] The geometries were optimized at the DFT/B3LYP level using a 6-31G(d,p) basis set. TDDFT calculations were performed using the B3LYP/6-311++G(d,p) method.

Fluorescence lifetime experiments

Fluorescence lifetime experiments were performed using a Horiba Jobin Yvon instrument in a Time-Correlated Single Photon Counting (TCSPC). A nano-LED of 390 nm was used as the source of excitation for **PYJO4**. LUDOX AS40 colloidal silica scattering medium was used for instrument response function.

Cell culture

Human breast adenocarcinoma MCF-7 cells were obtained from the American Type Culture Collection (ATCC), resuscitated from early passage liquid nitrogen vapour stocks as needed and cultured according to the supplier's instructions.

Confocal microscopy

Cells were seeded on cover slips one day before imaging. The next day cells were incubated with 30 μM **PYJO4** in RPMI 1640 (0.1% DMSO) without phenol red (Gibco) for 6 h at 37 °C, then washed with Hanks' balanced salt solution (HBSS) two times and after that treated with or without 40 μM $Hg(ClO_4)_2$ in RPMI without phenol red for 30 min at 37 °C. After washing with HBSS, cells were mounted with mounting medium on glass slides and viewed under an inverted confocal laser scanning microscope (Lieca, Germany). A Plan Apochromat 63×/1.4 NA Oil DIC objective lens was used for imaging and data collection. Green channel: λ_{ex} = 405 nm, λ_{em} = 500–570 nm. Red channel: λ_{ex} = 488 nm, λ_{em} = 600 nm long pass. Further, fluorescence intensity was quantified using image J software (Image J, National Institute of Health, Bethesda, MD).

Cytotoxicity assay

A standard colorimetric SRB (sulforhodamine B) assay was used for the measurement of cell viability as described before.[12,13] Briefly, 10 000–20 000 cells (depending on the doubling time of each cell type) were seeded to each well of a 96-well plate in 5% serum containing growth medium and incubated overnight in a CO_2 incubator at 37 °C. Adhered cells were then treated with the vehicle or compound at the required dose. After 48 hours of exposure, cells were fixed with ice-cold 50% TCA, stained with 0.4% (w/v) SRB in 1% acetic acid, washed and air dried. The bound dye was dissolved in 10 mM Tris base and the absorbance was measured at 510 nm on a plate reader (Epoch microplate reader, Biotek, USA). The cytotoxic effects of the compound were calculated as % cell viability as per the formula 100 − [100 − (absorbance of treated cells/absorbance of vehicle treated cells)] × 100.

Results and discussion

Molecular design and synthesis

Julolidine is an important chromophore which upon fusion with the 2-pyranone ring constitutes the pyranojulolidin-2-one framework. The remarkable fluorescence properties of pyrano[3,2-*f*]julolidin-2-ones are known in the literature,[14] however none has synthesized the related pyrano[3,2-*c*]julolidin-2-one (**PYJO**) class of compounds prior to this study. In an attempt to synthesize pyrano[3,2-*c*]julolidin-2-one **3** (**PYJO1**), julolidin-1-one[15] (**1**) was reacted with an easily accessible precursor α-oxo-ketene-*S*,*S*-acetal (**2**),[16] as shown in Scheme 1. Furthermore, the methylsulfanyl group of **PYJO1** was replaced by the *N*-methyl ethanolamine donor to fabricate the TICT based fluorophore **4** (**PYJO2**). The hydroxyl group of **PYJO2** was chloroacetylated using DMAP as base in dry DCM to give **5** (**PYJO3**). The dipicolyl amine chelator was then attached to the fluorophore **PYJO3** to furnish pyrano[3,2-*c*]julolidin-2-one **6** (**PYJO4**) in good yield.

Photophysical studies of synthesized pyrano[3,2-*c*]julolidin-2-ones

The absorption and emission characteristics of compounds **PYJO1–PYJO4** were investigated in methanol/HEPES buffer (7 : 3) at pH 7.2. The methylsulfanyl substituted **PYJO1** showed two absorption bands with maxima at 340 nm and 540 nm but did not show any fluorescence in the visible region (Fig. S1, ESI†). Fluorophores **PYJO2–PYJO4** exhibited two absorption bands centered at 330 nm and 460–470 nm for π–π* transition

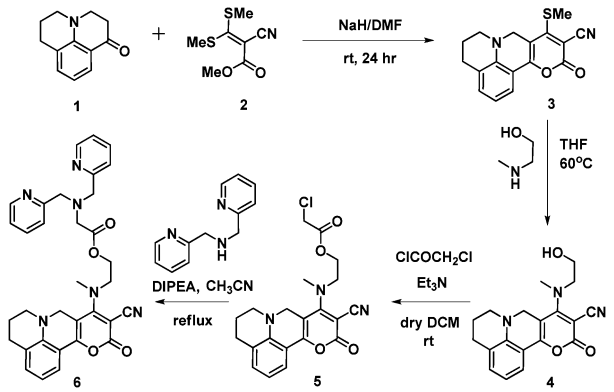

Scheme 1 Synthesis of pyranojulolidin-2-ones.

and n–π* transition, respectively (Fig. 2a). The fluorescence spectra of **PYJO2–PYJO4** revealed dual emission bands centered at 481–530 nm (green region) and 645–680 nm (red region) (Fig. 2b). It is noteworthy that **PYJO4** showed sharp dual-emission characteristics with a high intensity band in the NIR region possibly due to the effective TICT state.

DFT calculations of PYJO4

To understand the electronic behaviour of **PYJO4** in the ground state, the geometries were optimized at the DFT/B3LYP level using a 6-31G(d,p) basis set and time-dependent density functional theory (TDDFT) calculations were performed using the B3LYP/6-311++G(d,p) method. Fig. 2c shows the theoretically computed molecular orbitals in the ground states for **PYJO4**. The energies of the HOMO and LUMO levels, HOMO–LUMO gap, main orbital transition, and oscillator strength (*f*) are listed in Table S2, ESI.† The HOMO–LUMO charge density distribution for **PYJO4** reveals an effective charge transfer from the electron donating julolidine moiety to the electron withdrawing pyranone ring.

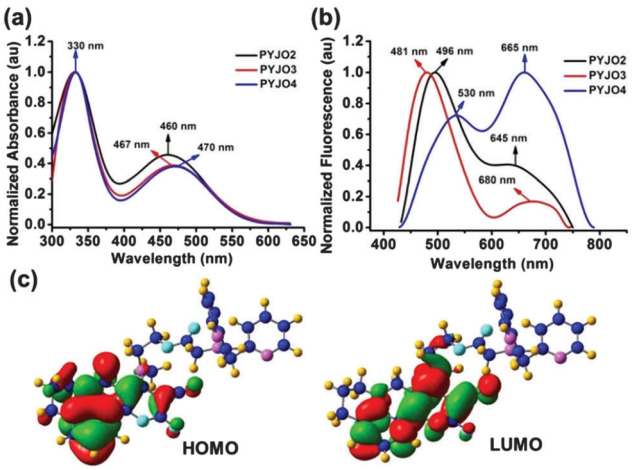

Fig. 2 (a) Normalized absorbance and (b) normalized fluorescence spectra of **PYJO2**, **PYJO3**, and **PYJO4** (4×10^{-5} M in methanol/HEPES buffer (7 : 3), pH 7.2) at λ_{ex} = 405 nm. (c) Computed molecular orbital energy diagrams and isodensity surface plots of **PYJO4** as obtained from TDDFT calculations.

Metal ion selectivity and test strip experiments

Dipicolylamine is a versatile host molecule that binds to a variety of metal ions with strong affinity depending upon the nature and point of attachment on the substrate.[9] Therefore, to test the metal ion selectivity for **PYJO4**, the photophysical studies were conducted in the presence of high concentration (10 equiv.) of perchlorate salts of Li^+, Na^+, K^+, Cs^+, Mg^{2+}, Ca^{2+}, Ba^{2+}, Cr^{3+}, Co^{2+}, Mn^{2+}, Fe^{2+}, Fe^{3+}, Cu^+, Cu^{2+}, Al^{3+}, Zn^{2+}, Pb^{2+}, Cd^{2+}, Hg^{2+} and Ni^{2+} ions. These experiments revealed that only Hg^{2+} triggered a dramatic increase in the emission ratio I_{530}/I_{665}, while other metal ions were either silent or induced a minor response (Fig. 3a). In order to confirm the binding of **PYJO4** exclusively with +2 oxidation state of mercury, the selectivity experiment of **PYJO4** was conducted using elemental mercury (Hg^0) and Hg^{1+} under similar conditions. **PYJO4** was found to be selective towards the Hg^{2+} species only (Fig. S2, ESI†), while no response was observed with other mercury ions (Hg^0 and Hg^+). The time-dependent fluorescence response of **PYJO4** for complexation with Hg^{2+} was also evaluated. The emission ratio I_{530}/I_{665} was immediately enhanced up to the maximum (~4.2 fold) after the addition of Hg^{2+} and remained invariable over an extended period of time (Fig. S3, ESI†). This experiment shows the strong affinity of the probe towards Hg^{2+}. We further conducted competitive experiments of **PYJO4** in the presence of higher concentration (10 mM each) of cellular ligands like cysteine (Cys), methionine (Met) and glutathione (GSH), which are found in abundance in cells. We observed that these ligands did not interfere with the complex of **PYJO4** and Hg^{2+} (Fig. S4, ESI†). The selectivity of the probe for Hg^{2+} ion prompted us to develop a simple, rapid and portable method for Hg^{2+} detection in contaminated water. The test strips coated with **PYJO4** were dipped into the aqueous solutions of different metal ions as shown in Fig. 3b. A distinct fluorescence change (red to green) was observed only in the case of Hg^{2+} ions. Furthermore, to check the sensitivity of **PYJO4** coated test strips for the detection of Hg^{2+} ions, we carried out concentration dependent experiments as shown in Fig. S5 (ESI†). Interestingly these **PYJO4** coated test strips could successfully detect Hg^{2+} ions up to the level of 200 ppb. Such an easy test for the

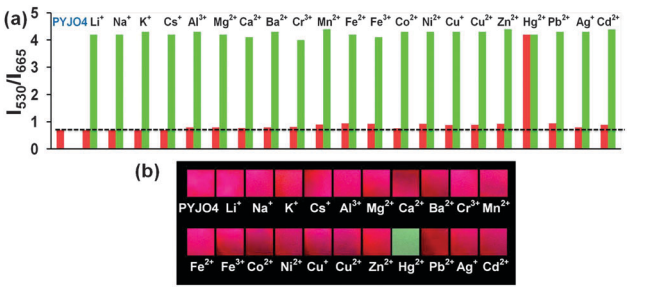

Fig. 3 (a) Selectivity studies of **PYJO4** (4×10^{-5} M) using a series of metal ions (10 equiv.) in methanol/HEPES buffer (7 : 3) at pH 7.2, λ_{ex} = 405 nm. Red bars: intensity ratio (I_{530}/I_{665}) in the absence or presence of a series of metal ions. Green bars: intensity ratio (I_{530}/I_{665}) of **PYJO4** in the presence of metal ions and Hg^{2+}, (b) Dip-stick test of **PYJO4** with different metal ions under a UV lamp (365 nm).

detection of Hg^{2+} ions in aqueous solution may be useful for monitoring the presence of this toxic metal ion.

Detailed ratiometric Hg^{2+} binding study and LOD measurements

To investigate the stoichiometry, binding affinity and detection limits of **PYJO4** for Hg^{2+} ions, the photophysical studies were conducted with increasing concentrations of Hg^{2+} ions. The buffered solution of **PYJO4** exhibited an absorption maximum at 330 nm (π–π^* transition) with a low intensity band at 470 nm (n–π^* transition), which gradually decreased upon the addition of Hg^{2+} ions (Fig. 4a). In the emission spectrum, two emission bands were observed, one at a shorter wavelength with maximum at 530 nm (green band) and the other at a longer wavelength with maximum at 665 nm (red band). Upon addition of Hg^{2+} ions the red band gradually decreased, while the green band increased with higher intensity. The ratiometric response of fluorescence intensities (I_{530}/I_{665}) enhanced from 0.7 to 4.2 with a final enhancement factor upto 6 fold. The titration studies with **PYJO4** revealed a good linearity between the fluorescence intensity ratio (Fig. S6 and S7, ESI†) and Hg^{2+} ion concentration with a detection limit of approximately 5.7×10^{-9} M (1.14 ppb) (Fig. S8, ESI†) which is below the permissible limits (2 ppb) in drinking water[17] as per the US Environmental Protection Agency and US Food and Drug Administration. Furthermore, Job's plot[18] established a 1 : 1 binding stoichiometry with Hg^{2+} ions (Fig. S9, ESI†). The binding constant ($\log \beta$) of **PYJO4** with Hg^{2+} ions was found to be 5.5 ± 0.8 by the non-linear least square fit of the absorbance titration data for the 1 : 1 model using Hypspec[19] software which was further analyzed by the corresponding fluorescence titrations (Fig. S10 and S11, ESI†). In order to exemplify the reversibility of probe **PYJO4** a solution of KI was added to the **PYJO4**–Hg^{2+} complex and it was found that the ratiometric sensing behaviour was successfully reversed with the appearance of the red band (Fig. S12, ESI†). Considering the relevance of pH in biological and environmental samples, the intensity ratio of probe **PYJO4** at different pH values (2–11) was studied which revealed negligible interference within pH 5–9 but a successive deviation in the intensity ratio was observed beyond this range (Fig. S13, ESI†).

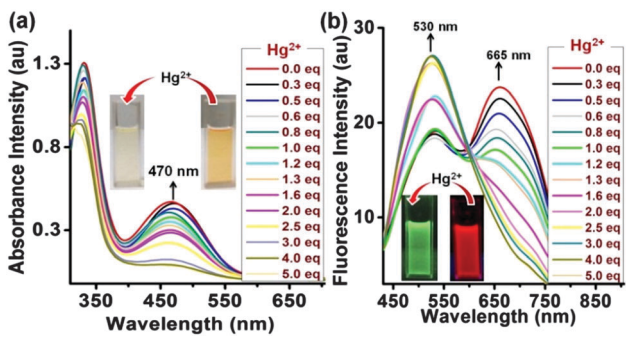

Fig. 4 (a) Absorption spectra with colorimetric images in visible light and (b) ratiometric fluorescence spectra of **PYJO4** upon addition of increasing concentrations of Hg^{2+} (0–5 equiv.) in methanol/HEPES buffer (7 : 3) at pH 7.2, λ_{ex} = 405 nm with fluorescence images.

Mechanistic studies of Hg^{2+} binding *via* twisted intramolecular charge transfer (TICT)

In order to confirm the TICT mechanism of **PYJO4**, the classical solvent viscosity and polarity experiments were conducted.[7,8] On increasing the solvent viscosity with ethylene glycol the rate of intramoleular rotation from LE to TICT states was restricted leading to an increase in the intensity of the planar LE state (green band) with the decrease in intensity of the TICT band (red band) (Fig. 5a). Furthermore, the absorption and fluorescence spectra were measured in solvents of varying polarity (Fig. S14 and Table S3, ESI†). There was no significant variation in the absorption spectra of **PYJO4** in different solvents. In the fluorescence spectra, a single-emission band was prominent in non-polar solvents, while a dual band was observed in polar solvents. These experiments confirmed the TICT behaviour of **PYJO4**.

Upon addition of Hg^{2+} ions to the solution of **PYJO4**, the binding of Hg^{2+} to the DPA moiety of the probe induced a change from the twisted state to the planar state resulting in the gradual decrease of the red band (665 nm) and subsequent increase of the green band (530 nm) (Fig. 5b). To get an insight into the excited state of probe **PYJO4** and **PYJO4**–Hg^{2+} complex, the time-resolved fluorescence experiment using time-correlated single photon counting (TCSPC) technique was carried out. As shown in Fig. S15 and Table S4 (ESI†), the fluorescence decay curve of **PYJO4** exhibited average life times of 7.08 ns and 3.36 ns corresponding to the two emission bands at 530 nm (LE state) and 665 nm (TICT state), respectively. However, upon addition of Hg^{2+} ion, the average life time of the green band in **PYJO4**–Hg^{2+} complex was found to 4.52 ns, which may be due to reorientation of the probe upon binding to Hg^{2+}. Thus, the results indicated the TICT behaviour of the probe **PYJO4**.

Ratiometric live cell imaging and quantification study

The aqueous compatibility and selectivity of **PYJO4** for Hg^{2+} over other biologically relevant metal cations (Na^+, K^+, Fe^{2+}, Ca^{2+}, Mg^{2+}, Zn^{2+}, Co^{2+}, Cu^{2+}) prompted us to apply **PYJO4** for the ratiometric fluorescence imaging of Hg^{2+} ions in live MCF-7 breast cancer cells. The cells incubated with **PYJO4** (30 μM, 0.1% DMSO in phenol red free RPMI medium without serum) exhibited intense intracellular fluorescence in the green channel (band pass 500–570 nm, Fig. 6B and C) and red channel (long pass 600 nm, Fig. 6D and E) in accordance with the dual

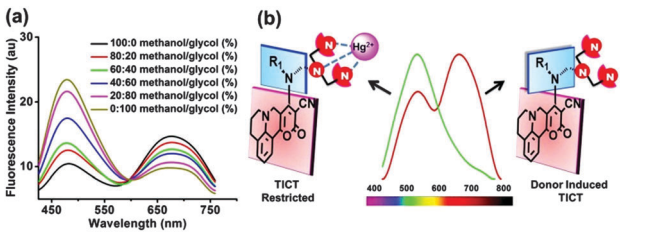

Fig. 5 (a) Normalized fluorescence emission spectra of **PYJO4** (4×10^{-5} M) in methanol/ethylene glycol. λ_{ex} = 405 nm. (b) Predicted binding mechanism of **PYJO4**.

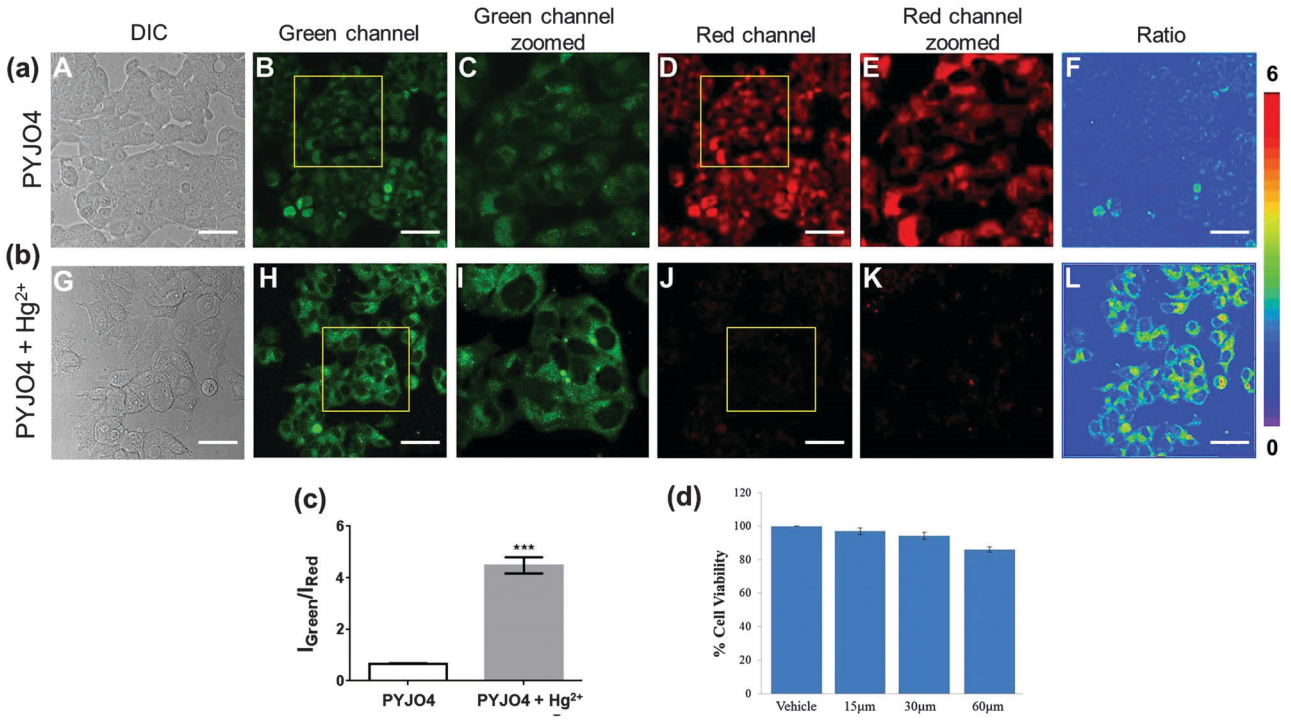

Fig. 6 (a) MCF-7 cells incubated with **PYJO4** (3×10^{-5} M, 6 h). (b) MCF-7 cells incubated with **PYJO4** followed by $Hg(ClO_4)_2$ (4×10^{-5} M, 30 min) supplementation. (c) Ratiometric quantification of relative fluorescence intensity using image J software, ***$p < 0.001$. Green channel: λ_{ex} = 405 nm, λ_{em} = 500–570 nm. Red channel: λ_{ex} = 488 nm, λ_{em} = 600 nm long pass. Each experiment was repeated three independent times. Error bars are ± s.e.m. (n = 3). Statistical analysis was performed using student's t test. Scale bar: 50 μm. (d) MTT assay of **PYJO4** at different concentrations.

fluorescence band observed in photophysical studies (Fig. S16, ESI†). Furthermore, MCF-7 cells pretreated with **PYJO4** followed by washing and then treatment with $Hg(ClO_4)_2$ (40 μM, 30 min) showed a significant increase in intracellular fluorescence in the green channel (Fig. 6H and I) due to the formation of the **PYJO4**–Hg^{2+} complex, whereas no fluorescence was observed in the red region (Fig. 6J and K). The ratiometric fluorescence images (Fig. 6F and L) revealed a significant increase in the intracellular green to red intensity ratio (I_{green}/I_{red}) in the presence of Hg^{2+} ions (Fig. 6c) suitable for the ratiometric quantification of intracellular Hg^{2+} ions. **PYJO4** showed no cytotoxicity under the conditions used for cell imaging (Fig. 6d). Therefore, the live cell imaging studies demonstrated that **PYJO4** can be successfully utilized for the ratiometric detection and imaging of intracellular Hg^{2+} ions in live cancer cells.

Conclusions

In conclusion, we have rationally designed and developed a ratiometric fluorescent molecular rotor **PYJO4** based on a novel pyrano[3,2-*c*]julolidin-2-one scaffold operating *via* a TICT mechanism for selective detection of Hg^{2+} ions. We have successfully demonstrated the application of **PYJO4** for the detection and ratiometric imaging of intracellular Hg^{2+} in live MCF-7 breast cancer cells. **PYJO4** exhibited impressive sensitivity (1.14 ppb) towards Hg^{2+} ions. The probe can be employed as a test strip for the detection of toxic Hg^{2+} ions in contaminated water. The probe has opened new avenues for deciphering the biotoxicity mechanism associated with Hg^{2+} ions. Further studies in this direction are currently under way.

Acknowledgements

AG thanks the Department of Atomic Energy (DAE-SRC) for the Outstanding Investigator Award (21/13/2015-BRNS/35029). The authors thank CSIR, New Delhi, for research support. We acknowledge SAIF-CDRI for providing spectral data and Mrs Rima A. Sarkar for confocal images. We are grateful to Prof. A. K. Mishra, IIT Madras, Chennai, for time-resolved fluorescence measurements. The CDRI communication number is 9258.

Notes and references

1 (*a*) WHO fact sheet on Mercury and Health, 2016, http://www.who.int/mediacentre/factsheets/fs361/en/; (*b*) H. H. Harris, I. J. Pickering and G. N. George, *Science*, 2003, **301**, 1203; (*c*) B. Weiss, *Toxicol. Sci.*, 2007, **97**, 223.
2 H. L. Needleman, *JAMA*, 2006, **295**, 1835.
3 (*a*) S. B. Maity, S. Banerjee, K. Sunwoo, J. S. Kim and P. K. Bharadwaj, *Inorg. Chem.*, 2015, **54**, 3929; (*b*) X. Zhou, X. Wu and J. Yoon, *Chem. Commun.*, 2015, **51**, 111; (*c*) R. Bhowmick, R. Alam, T. Mistri, D. Bhattacharya, P. Karmakar and M. Ali, *ACS Appl. Mater. Interfaces*, 2015, **7**, 7476; (*d*) E. Karakuş, M. Üçüncü and M. Emrullahoğlu,

Chem. Commun., 2014, **50**, 1119; (*e*) P. Srivastava, S. S. Razi, R. Ali, R. C. Gupta, S. S. Yadav, G. Narayan and A. Misra, *Anal. Chem.*, 2014, **86**, 8693; (*f*) D. T. Quang and J. S. Kim, *Chem. Rev.*, 2010, **110**, 6280; (*g*) H. N. Kim, W. X. Ren, J. S. Kim and J. Yoon, *Chem. Soc. Rev.*, 2012, **41**, 3210; (*h*) Z. Guo, S. Park, J. Yoon and I. Shin, *Chem. Soc. Rev.*, 2014, **43**, 16; (*i*) J. Liu, Y. Q. Sun, P. Wang, J. Zhang and W. Guo, *Analyst*, 2013, **138**, 2654; (*j*) Y. Wei, D. Cheng, T. Ren, Y. Li, Z. Zeng and L. Yuan, *Anal. Chem.*, 2016, **88**, 1842; (*k*) G. Niu, W. Liu, J. Wu, B. Zhou, J. Chen, H. Zhang, J. Ge, Y. Wang, H. Xu and P. Wang, *J. Org. Chem.*, 2015, **80**, 3170; (*l*) Z. Guo, W. Zhu, M. Zhu, X. Wu and H. Tian, *Chem. – Eur. J.*, 2010, **16**, 14424; (*m*) Y. Jiao, L. Zhang and P. Zhou, *Talanta*, 2016, **150**, 14; (*n*) X. Chen, X. Meng, S. Wang, Y. Cai, Y. Wu, Y. Feng, M. Zhu and Q. Guo, *Dalton Trans.*, 2013, **42**, 14819; (*o*) C. Jiang, Z. Guan, S. Y. R. Lim, L. Polavarapu and Q. H. Xu, *Nanoscale*, 2011, **3**, 3316; (*p*) L. PolavarapuJ. Pérez-JusteQ. H. XuL. M. Liz-Marzán *J. Mater. Chem. C*2014, **2**, 7460.

4 (*a*) Y. X. Hou, Q. J. Lu, J. H. Deng, H. T. Li and Y. Y. Zhang, *Anal. Chim. Acta*, 2015, **866**, 69; (*b*) K. Kanagaraj, K. Bavanidevi, T. J. Chow and K. Pitchumani, *RSC Adv.*, 2014, **4**, 11714.

5 (*a*) E. A. Lemke and C. Schultz, *Nat. Chem. Biol.*, 2011, **7**, 480; (*b*) S. Maruyama, K. Kikuchi, T. Hirano, Y. Urano and T. Nagano, *J. Am. Chem. Soc.*, 2002, **124**, 10650.

6 (*a*) E. M. Nolan and S. J. Lippard, *J. Mater. Chem.*, 2005, **15**, 2778; (*b*) E. M. Nolan and S. J. Lippard, *J. Am. Chem. Soc.*, 2007, **129**, 5910; (*c*) E. M. Nolan and S. J. Lippard, *Chem. Rev.*, 2008, **108**, 3443; (*d*) X. Zhang, Y. Xiao and X. Qian, *Angew. Chem., Int. Ed.*, 2008, **47**, 8025; (*e*) H. B. Li and H. J. Yan, *J. Phys. Chem. C*, 2009, **113**, 7526; (*f*) M. Suresh, S. Mishra, S. K. Mishra, E. Suresh, A. K. Mandal, A. Shrivastav and A. Das, *Org. Lett.*, 2009, **11**, 2740; (*g*) X. Cheng, Q. Li, J. Qin and Z. Li, *ACS Appl. Mater. Interfaces*, 2010, **2**, 1066; (*h*) B. Gu, L. Huang, N. Mi, P. Yin, Y. Zhang, X. Tu, X. Luo, S. Luo and S. Yao, *Analyst*, 2015, **140**, 2778; (*i*) G. Chen, Z. Guo, G. Zeng and L. Tang, *Analyst*, 2015, **140**, 5400.

7 (*a*) E. Lippert, W. Leuder, F. Moll, H. Nagele, H. Boos, H. Prigge and I. Siebold-Blankenstein, *Angew. Chem.*, 1961, **73**, 695; (*b*) Z. R. Grabowski and K. Rotkiewicz, *Chem. Rev.*, 2003, **103**, 3899.

8 (*a*) M. A. Haidekker, T. P. Brady, D. Lichlyter and E. A. Theodorakis, *J. Am. Chem. Soc.*, 2006, **128**, 398; (*b*) W. L. Goh, M. Y. Lee, T. L. Joseph, S. T. Quah, C. J. Brown, C. Verma, S. Brenner, F. J. Ghadessy and Y. N. Teo, *J. Am. Chem. Soc.*, 2014, **136**, 6159; (*c*) Z. Yang, J. Cao, Y. He, J. H. Yang, T. Kim, X. Peng and J. S. Kim, *Chem. Soc. Rev.*, 2014, **43**, 4563; (*d*) S. Umar, A. K. Jha and A. Goel, *Asian J. Org. Chem.*, 2016, **5**, 187.

9 (*a*) C. C. Woodroofe and S. J. Lippard, *J. Am. Chem. Soc.*, 2003, **125**, 11458; (*b*) L. Xue, C. Liu and H. Jiang, *Org. Lett.*, 2009, **11**, 1655; (*c*) S. Mizukami, S. Okada, S. Kimura and K. Kikuchi, *Inorg. Chem.*, 2009, **48**, 7630; (*d*) J. Hataia and S. Bandyopadhyay, *Chem. Commun.*, 2014, **50**, 64; (*e*) Q. Li, M. Peng, H. Li, C. Zhong, L. Zhang, X. Cheng, X. Peng, Q. Wang, J. Qin and Z. Li, *Org. Lett.*, 2012, **14**, 2094.

10 Y. Tominaga, *Trends Heterocycl. Chem.*, 1991, **2**, 43.

11 M. J. Frisch, G. W. Trucks, H. B. Schlegel, G. E. Scuseria, M. A. Robb, J. R. Cheeseman, G. Scalmani, V. Barone, B. Mennucci, G. A. Petersson, H. Nakatsuji, M. Caricato, X. Li, H. P. Hratchian, A. F. Izmaylov, J. Bloino, G. Zheng, J. L Sonnenberg, M. Hada, M. Ehara, K. Toyota, R. Fukuda, J. Hasegawa, M. Ishida, T. Nakajima, Y. Honda, O. Kitao, H. Nakai, T. Vreven, J. A. Montgomery, Jr., J. E. Peralta, F. Ogliaro, M. Bearpark, J. J. Heyd, E. Brothers, K. N. Kudin, V. N. Staroverov, R. Kobayashi, J. Normand, K. Raghavachari, A. Rendell, J. C. Burant, S. S. Iyengar, J. Tomasi, M. Cossi, N. Rega, N. J. Millam, M. Klene, J. E. Knox, J. B. Cross, V. Bakken, C. Adamo, J. Jaramillo, R. Gomperts, R. E. Stratmann, O. Yazyev, A. J. Austin, R. Cammi, C. Pomelli, J. W. Ochterski, R. L. Martin, K. Morokuma, V. G. Zakrzewski, G. A. Voth, P. Salvador, J. J. Dannenberg, S. Dapprich, A. D. Daniels, Ö. Farkas, J. B. Foresman, J. V. Ortiz, J. Cioslowski and D. J. Fox, *Gaussian 09, revision A.02*, Gaussian, Inc., Wallingford, CT, 2009.

12 V. Vichai and K. Kirtikara, *Nat. Protoc.*, 2006, **1**, 1112.

13 S. S. Chauhan, A. K. Singh, S. Meena, M. Lohani, A. Singh, R. K. Arya, S. H. Cheruvu, J. Sarkar, J. R. Gayen and D. Datta, *Bioorg. Med. Chem. Lett.*, 2014, **24**, 2820.

14 (*a*) N. C. Lim and C. Brückner, *Chem. Commun.*, 2004, 1094; (*b*) L. Yuan, W. Lin, J. Song and Y. Yang, *Chem. Commun.*, 2011, **47**, 12691; (*c*) H. S. Jung, K. C. Ko, J. H. Lee, S. H. Kim, S. Bhuniya, J. Y. Lee, Y. Kim, S. J. Kim and J. S. Kim, *Inorg. Chem.*, 2010, **49**, 8552; (*d*) D. R. Rooker and D. Buccella, *Chem. Sci.*, 2015, **6**, 6456.

15 T. A. Crabb and S. L. Soileux, *Tetrahedron*, 1986, **42**, 5407.

16 (*a*) H. Junjappa, H. Ila and C. V. Asokan, *Tetrahedron*, 1990, **46**, 5423; (*b*) A. Goel, A. Sharma, M. Kathuria, A. Bhattacharjee, A. Verma, P. R. Mishra, A. Nazir and K. Mitra, *Org. Lett.*, 2014, **16**, 756; (*c*) A. Goel, S. Umar, P. Nag, A. Sharma, A. Nazir, L. Kumar, Shamsuzzama, J. R. Gayen and Z. Hossain, *Chem. Commun.*, 2015, **51**, 5001; (*d*) A. Sharma, S. Umar, P. Kar, K. Singh, M. Sachdev and A. Goel, *Analyst*, 2016, **141**, 137.

17 (*a*) United States FDA Code of Federal Regulations, 21CFR165.110, 2015; (*b*) United States Environmental Protection Agency Roadmap for Mercury, EPA-HQ-OPPT-2005-0013, 2006.

18 H. Zheng, X.-J. Zhang, X. Cai, Q.-N. Bian, M. Yan, G.-H. Wu, X.-W. Lai and Y.-B. Jiang, *Org. Lett.*, 2012, **14**, 1986.

19 P. Gans, A. Sabatini and A. Vacca, *Talanta*, 1996, **43**, 1739.

